B. DIFFUSION-CELL EXPERIMENTS

Experimental Procedures and Data Analysis

We constructed diffusion cells with two chambers containing groundwater separated by a slab of tuff. After radioactive tracers were added to one of the chambers, we periodically monitored the untraced chamber for the presence of radioactivity by taking an aliquot of the solution in the chamber and then replenishing that chamber with groundwater. The dimensions of the diffusion cells we used are given in Table 35.

Table 35. Dimensions of Diffusion Cells

Diameter of tuff slab	6 cm
Length of tuff slab	1 cm
Volume of traced chamber	750 cm^3
Volume of untraced chamber	80 cm^3

The only driving force in this experimental setup is the chemical concentration gradient; thus, the solute flux is purely diffusive. The apparent time of arrival depends on the porosity, the heterogeneity of the pore structure, the retardation factor for a given radionuclide, and the sensitivity of radionuclide measurements. The rate of concentration increase in the untraced chamber depends on the ionic diffusivity, the tuff porosity, and the tuff tortuosity/constrictivity factor. Thus, by measuring the movement of sorbing and nonsorbing tracers through tuff slabs as a function of time, we can measure the rock-dependent diffusion parameters.

The two major rock types used for the diffusion-cell experiments were zeolitic (UE-25 1362) and devitrified (G4-287). The zeolitic tuff has a porosity of 0.4 and a bulk density of 1.5 ml/g. The devitrified tuff has a porosity of 0.2 and a bulk density of 2.3 ml/g. The major component of the zeolitic tuff is clinoptilolite; the major component of the devitrified tuff is alkali feldspar.

The solutions used for the diffusion-cell experiments were prepared by taking an aliquot of a ^{3}H, ^{95m}Tc, natural U(VI), $^{237}Np(V)$, or $^{239}Pu(V)$ acidic stock and diluting it in the water being studied. The actinide concentration of the solutions used for the diffusion experiments was very close to the solubility limit of the actinides in the groundwaters. The experimentally determined solubilities (Nitsche et al. 1993a, 1994) of plutonium range from 2×10^{-7} (J-13 water at a pH of 7) to 1×10^{-6} M (UE-25 p#1 water at a pH of 8.5) and of neptunium range from 7×10^{-6} (UE-25 p#1 water at a pH of 8.5) to 5×10^{-3} M (J-13 water at a pH of 6). Table 14 in Chapter IV summarizes the solubilities and speciation of neptunium in these groundwaters.

The experimental setup for the diffusion cells can be described by a one-dimensional diffusion model. Thus, Eqn. 64 in the section on rock-beaker experiments can be rewritten as

$$D_e \frac{\partial^2 C}{\partial x^2} = \alpha \frac{\partial C}{\partial t} \quad , \qquad (67)$$

where x is the the axis along the direction of tracer diffusion, D_e is the effective diffusivity ($= \epsilon\, d$), and α is the rock-capacity factor ($= \epsilon\, R_f$). This equation yields an analytic solution to diffusion through a slab.

Bradbury et al. (1986) solved Eqn. 67 for a porous rock. For our experimental setup, the boundary conditions can be taken to be

- at $x = 0$, a constant source concentration, C_o, is maintained, and
- at $x = \ell$, where ℓ is the tuff-slab thickness, the concentration measured at the initially untraced cell, C_t, is much smaller than the source concentration ($C_t \ll C_o$).

For these conditions, the total quantity, Q_t, diffused through a tuff slab of area A after a time t is given

by the equation

$$\frac{Q_t}{A\,\ell\,C_o} = \frac{D_e\,t}{\ell^2} - \frac{\alpha}{6} - \frac{2\alpha}{\pi^2}\sum_{n=1}^{\infty}\frac{(-1)^n}{n^2}e^{-\left(\frac{D_e n^2 \pi^2 t}{\ell^2 \alpha}\right)} . \quad (68)$$

As $t \to \infty$, the asymptotic solution becomes

$$Q_t = \frac{A\,C_o\,D_e}{\ell}\,t - \frac{A\,C_o\,\ell\,\alpha}{6} . \quad (69)$$

Consequently, a plot of Q_t versus t yields the effective diffusivity, D_e, from the slope and the rock-capacity factor, α, from the intercept on the time axis of the extrapolated linear region. For a non-sorbing species, $K_d = 0$, $R_f = 1$, and $\alpha = \epsilon$; for a sorbing species, K_d may be calculated from the value of α.

The diffusion coefficient, d, can be calculated from the effective diffusivity ($D_e = \epsilon\, d$). The difference between the diffusion coefficient, d_s, for a tracer diffusing through the solution phase and the diffusion coefficient, d, for a tracer passing through tuff pores is given by

$$d = \frac{\delta}{\tau^2}\,d_s , \quad (70)$$

where δ is the constrictivity and τ is the tortuosity of the tuff pore structure.

Results and Discussion

We studied the diffusion of ^{3}H, ^{95m}Tc, natural U(VI), ^{237}Np(V), and ^{239}Pu(V) through devitrified and zeolitic tuffs using water from Well J-13 and synthetic UE-25 p#1 water. The radionuclides ^{3}H, natural U(VI), and ^{239}Pu(V) were studied together in four diffusion cells (devitrified and vitric tuff cells, each with both types of water). Likewise, the radionuclides ^{95m}Tc and ^{237}Np(V) were studied together in another four diffusion cells. Typical results for these experiments are shown in the Figs. 133 through 135.

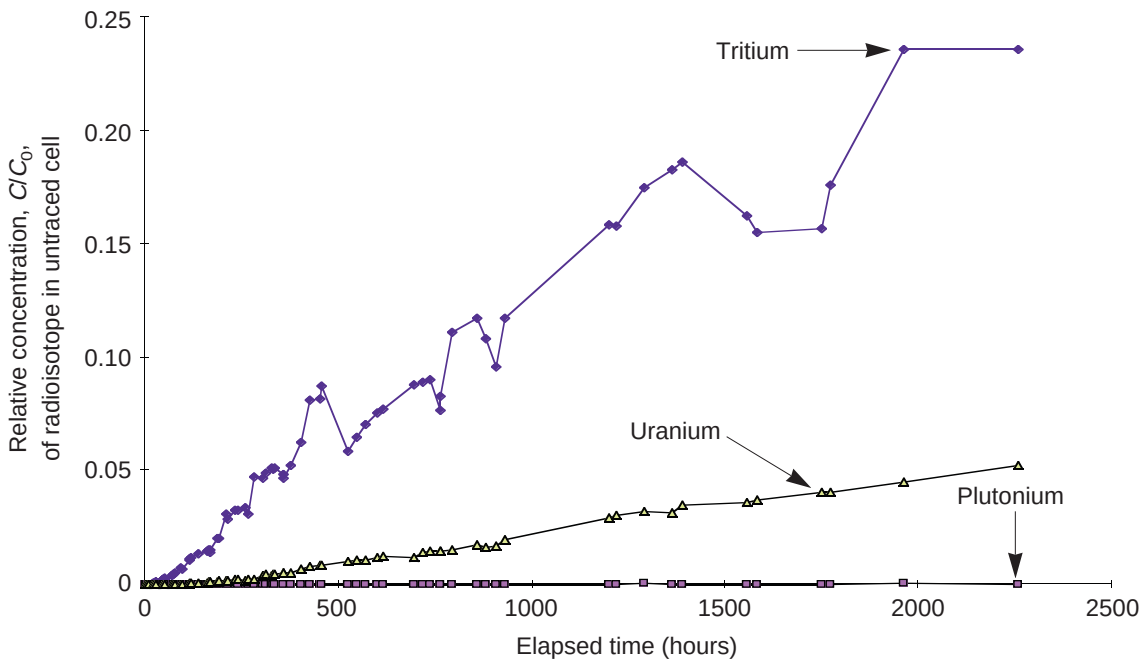

Figure 133. Tritium, Plutonium, and Uranium Diffusion through Devitrified Tuff. The data show the concentration in synthetic UE-25 p#1 water of ^{3}H, ^{239}Pu(V), and natural U(VI) (relative to the concentration in the traced cell, C/C_0) diffusing through devitrified tuff G4-287 into the untraced cell as a function of time.

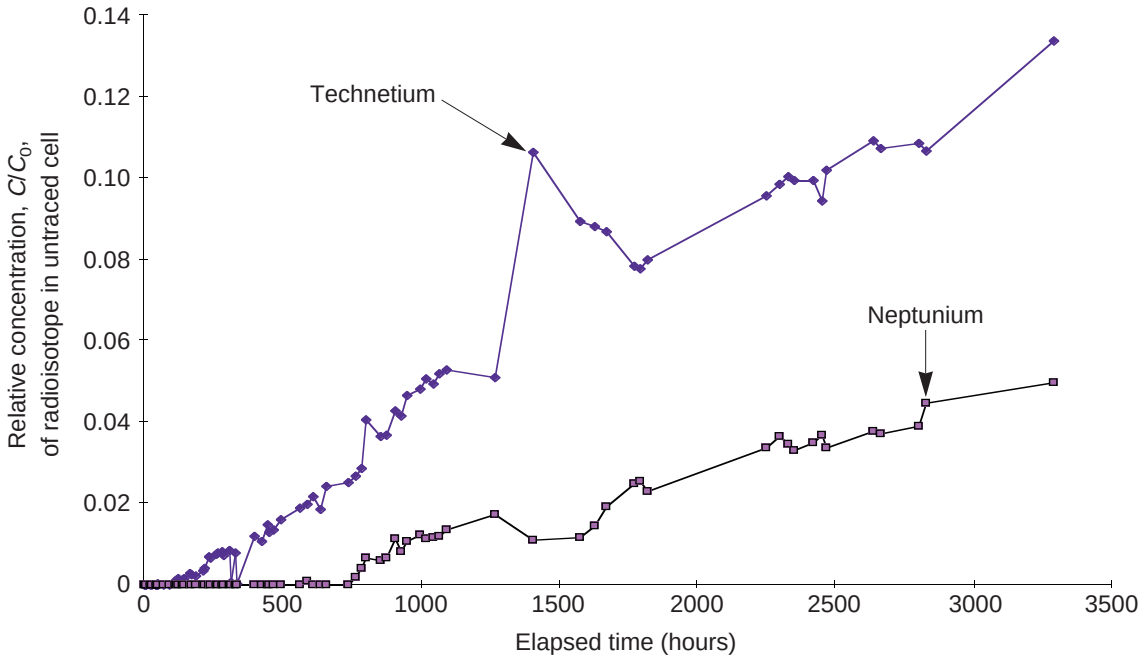

Figure 134. Technetium and Neptunium Diffusion through Devitrified Tuff. The data show the concentration in synthetic UE-25 p#1 water of ^{95m}Tc and ^{237}Np (relative to the concentration in the traced cell, C/C_0) diffusing through devitrified tuff G4-287 into the untraced cell as a function of time.

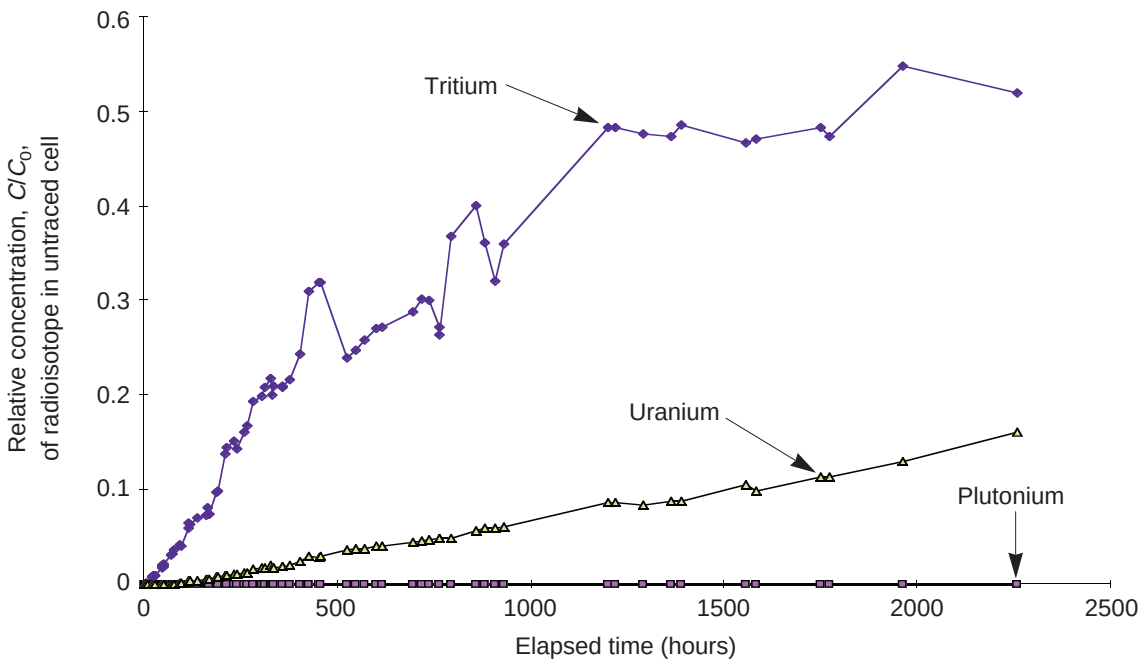

Figure 135. Tritium, Plutonium, and Uranium Diffusion through Zeolitic Tuff. The data show the concentration in synthetic UE-25 p#1 water of ^{3}H, ^{239}Pu(V), and natural U(VI) (relative to the concentration in the traced cell, C/C_0) diffusing through zeolitic tuff UE-25-1362 into the untraced cell as a function of time.

Our results indicate that the diffusion of nonsorbing radionuclides into saturated tuff (illustrated by the diffusion of tritiated water in Figs. 133 and 135) is slower in devitrified tuffs than in zeolitic tuffs. Large anions such as pertechnetate (which are excluded from the tuff pores by size and charge) diffuse slower through the pores than tritium regardless of the groundwater or tuff type (as also observed in the rock-beaker experiments). The migration of plutonium through tuff under diffusive conditions is dominated by sorption (as shown by Figs. 133 and 135). The migration of Np(V) and U(VI) through tuff depends on tuff type and water chemistry. In cases, such as tuff G4-287 in Figs. 133 and 134, for which the reported sorption of neptunium onto tuff is essentially zero (Triay et al. 1996a, 1996b), the diffusion of neptunium through the tuff is slower than the diffusion of tritium but comparable to the diffusion of a nonsorbing, large anion, such as pertechnetate (Fig. 134).

The analysis of data described in the "Experimental Procedures and Data Analysis" section of this chapter has some problems with respect to the assumptions required to find an analytical solution. The assumptions do not allow for a changing concentration in the traced chamber, for a concentration in the untraced chamber that is not much smaller than the initial concentration in the traced chamber, and for the addition of groundwater to the untraced chamber each time an aliquot was taken.

Therefore, future analysis of these data will involve fitting the diffusion profiles using a transport code (such as the TRACRN code used in the rock-beaker diffusion experiments) to obtain diffusion coefficients. The concentration profiles of the diffusing radionuclides would be fitted to the same equation as Eqn. 70 but using the algebraic form given in the section on rock-beaker experiments (Eqns. 61 through 63).